water

MDPI

Article

The Adsorptive Removal of Bengal Rose by Artichoke Leaves: Optimization by Full Factorials Design

Amel Khalfaoui [1], Mohamed Nadir Khelifi [2], Anouar Khelfaoui [1], Abderrezzaq Benalia [1,2], Kerroum Derbal [2], Corrado Gisonni [3], Gaetano Crispino [3] and Antonio Panico [3,*]

[1] LIPE Laboratory, Department of Environmental Engineering, Faculty of Engineering Process, University of Constantine 3, Constantine 2500, Algeria; khalfaoui_amel@yahoo.fr (A.K.); kelfaoui.anouar@gmail.com (A.K.); benalia.abderrezzak@gmail.com (A.B.)
[2] Laboratory of Process Engineering for Sustainable Development and Health Products (GPDDPS), National Polytechnic School of Constantine Department of Process, Engineering, Constantine 2500, Algeria; mohamed.nadir@outlook.fr (M.N.K.); derbal_kerroum@yaoo.fr (K.D.)
[3] Department of Engineering, University of Campania L. Vanvitelli, 81031 Aversa, Italy; corrado.gisonni@unicampania.it (C.G.); gaetano.crispino@unicampania.it (G.C.)
* Correspondence: antonio.panico1@unicampania.it; Tel.: +39-081-5010228

Abstract: Currently, the dye industry is increasing its production as a consequence of the growing need for their products in different manufacturing sectors, such as textiles, plastics, food, paper, etc... Thereafter, these industries generate very large volumes of effluents contaminated by these dyes, which require proper removal treatment before final discharge of the effluents into the environment. In this study, artichoke leaves were used as an economical and eco-friendly bio-adsorbent for Bengal Rose (BR) dye removal. Bio-adsorbent obtained from artichoke leaves was ground to powder size. The resulting powder was characterized by different methods, such as Brunauer-Emmett-Teller (BET) surface area analysis, scanning electron microscopy(SEM), X-ray Diffraction (XRD), Fourier transfer infrared (FTIR), pH at point of zero charge (pH_{pzc}), equilibrium pH, iodine number, methylene blue number, phenol number, density, Energy dispersive X-ray spectroscopy (EDX) and Thermo-gravimetric analysis (TGA). Thereafter, the bio-adsorbent was used to study its capability for removing BR dye by testing contact time, initial concentration of dye and temperature. The results show that the saturation of bio-sorbent was reached after 40 min and the removal rate of BR dye by artichoke leaves powder (ALP) was 4.07 mg/g, which corresponds to a removal efficiency of 80.1%. A design of experiences (DOE) based on a two-level full factorial design (2^3) was used to study the effects of different parameters, such as pH, temperature and bio-adsorbent dosage on BR dye removal efficiency. The obtained results show that the highest removal efficiency was 86.5% for the optimized values of pH (4), temperature (80 °C) and bio-adsorbent dosage (8 g/L). Furthermore, a satisfying accordance between experimental and predicted data was observed. The kinetic and isotherm studies show that the pseudo-second order model simulated adequately the obtained data and it was found that Langmuir and Temkin isotherm models are liable and suitable for evaluating the adsorption process performance. Free energy change of adsorption (ΔG°), enthalpy change (ΔH°) and entropy change (ΔS°) were furthermore calculated to predict the nature of the adsorption process.

Keywords: Bengal Rose; adsorption; artichoke leaves; water treatment; full factors design

Citation: Khalfaoui, A.; Khelifi, M.N.; Khelfaoui, A.; Benalia, A.; Derbal, K.; Gisonni, C.; Crispino, G.; Panico, A. The Adsorptive Removal of Bengal Rose by Artichoke Leaves: Optimization by Full Factorials Design. *Water* **2022**, *14*, 2251. https://doi.org/10.3390/w14142251

Academic Editor: Laura Bulgariu

Received: 8 June 2022
Accepted: 15 July 2022
Published: 18 July 2022

1. Introduction

A large quantity and variety of dyes are used in different industries, such as printing, food, textile, leather, cosmetic, dying, pharmaceuticals and petroleum [1,2]. Therefore, the effluents from these industries are loaded with dyes at varying concentrations [3,4]. Such wastewaters are generally discharged into the environment with an incomplete treatment or without any treatment at all, thus causing detrimental effects to the environment and aquatic life [5,6] as well as to human health [4,7] due to the presence of dyes [8].

Currently, several methods and processes are used to partially or completely remove dyes from different industrial effluents. Among them, coagulation combined with flocculation [9], precipitation [10], membrane processes filtration [11], advanced oxidation processes [12], adsorption [13], electro-coagulation [14] and electrochemical methods [15,16] are the most common.

In this work, the adsorption process has been tested as a method to remove dyes from wastewater thanks to its simplicity, high removal efficiency and low cost [17]. The adsorption method uses different types of adsorbents depending on the characteristics of molecules to be removed. From the international literature, the use of activated carbon to remove different types and sources of dyes is highly recommended. According to the literature, a wide range of dyes (e.g., methylene blue) can be removed by adsorbents obtained from natural materials such as vegetable wastes or clays, with removal efficiencies that can exceed 90% [18]. In a recently published study, waste pea shells were used as an adsorbent to remove phenol, with the highest uptake rate of 125.77 mg/g when the phenol concentration was 500 mg/L [19]. Moreover, low cost activated carbon obtained from *Polygonum orientale* Linn has shown high capacity to remove dyes, such as malachite green (MG) and rhodamine B (RB), with the highest removal efficiencies of 98.4% and 73.5%, respectively [20]. In addition, materials such as bottom ash (BA) from power plants and de-oiled soya (DOS)from the soya bean industry were used for crystal violet dye removal. The obtained results show that dye removal efficiencies of 95% and 78% were achieved from BA and DOS, respectively [21]. Finally, biomaterials from fruit waste such as banana and orange peels have been used successfully to remove methylene blue and copper (II) ions from wastewater;the removal efficiencies were 98.3% and 99%, respectively [22–24]. Among all the organic wastes that can be used to produce bio-absorbents, this work is focused on artichoke leaves, aiming to find for them a valuable recovery, as the edible part of artichoke approximately amounts to 40%, thus generating 60% of waste. Moreover, Algeria is considered one of the main green artichoke (*Cynara cardunculusvar. scolymus*)producing countries in the world, with 119,636 tons per year. Therefore, a considerable amount of waste is generated yearly after processing artichokes, which requires treatment or recovery before its final discharge into the environment. Therefore, the aim of the study is focused on recovering artichoke waste and making it suitable for water treatment methods.

Artichoke leaves have been tested by several researchers for the removal of a wide range of pollutants from water [25], and in particular from textile industry effluents [26], such as: (i) potentially toxic elements (e.g., Pb(II), Cd(II) and Cu(II) in aqueous solutions) [27]; (ii) anionic (methyl orange, MO) and cationic dyes (methylene blue, MB) [28]; and (iii) metformin hydrochloride anti-diabetic drugs. In this work, artichoke leaves were tested to remove Bengal Rose (BR) dye for the first time, thus opening new perspectives on the recovery of this waste as well as on the sustainable and low-cost removal of BR dye from wastewater without using chemicals that can leave residues on treated waters, thus limiting their reuse in different fields, such as irrigation, which is extremely relevant in arid countries such as Algeria.

The present work is structured into three main sections: (i) preparation of bio-adsorbent from artichoke leaves; (ii) bio-adsorbent characterization; and(iii) bio-adsorbent use to remove BR dye. A mathematical study based on a full factorial design model was furthermore used to assess the effects of different operating parameters such as temperature, pH and bio-adsorbent dosage on BR dye removal efficiency.

2. Materials and Methods

2.1. Raw Material and Chemical Reagents

Artichoke leaves used to prepare the bio-adsorbent were manually collected from household waste. BR ($C_{20}H_2Cl_4I_4Na_2O_5$, 973.67 g/mol) dye, with purity that exceeds 99%, was purchased from Sigma Aldrich Company (Chemie GmbH, Eschenstr. 5, 82024 Taufkirchen, Germany).

2.2. BR Solution

A stock solution of BR dye with an initial concentration of 0.5 g/L was prepared by dissolving 500 mg of dye powder in 1 L of distilled water. All the required experimental solutions were prepared using the stock solution by successive dilution as long as the desired concentration was achieved. The pH was adjusted by adding volumes of hydrochloric acid (HCl 0.1 or 1 N) and sodium hydroxide (NaOH 0.1 or 1 N) solutions. The pH measurement was performed with a calibrated pH meter (type 3510 JENWAY, Cambridge, UK). Standard solutions of BR dye were obtained from the stock solution and used to draw the calibration curves.

2.3. Bio-Adsorbent

With the aim of finding an inexpensive and efficient biomaterial for the removal of dyes from wastewater, artichoke leaves were chosen as a natural source to obtain biosorbents. The sequence used to obtain bio-adsorbents from artichoke leaves is reported as follows. First, the waste composed of artichoke leaves was washed with tap water and then with distilled water to remove residual impurities and soluble parts. The washing process was repeated several times until clear washing water was obtained. Next, the artichoke leaves were dried in an oven at a temperature of 50 °C for 72–96 h, as long as the mass was invariable. Then, the artichoke leaves were crushed using a grinder and sieved with 250 µm sieves. The last step was to dry the bio-adsorbent powder in an oven at a temperature of 50 °C for another 72–96 h, as long as the mass was invariable. After that, the obtained biomaterial in powder size was stored in desiccators for further use.

2.4. Methods

2.4.1. Bio-Adsorbent Characterization

For physical and chemical characterization of the bio-adsorbent, i.e., artichoke leaves in powder size (ALP), several techniques were used. A Brunauer-Emmett-Teller (BET) surface area analysis was used to measure the surface area using surface area analyser (Quantachrome Instruments Corporate Headquarters, Boynton Beach, FL, USA), a scanning electron microscopy (SEM) was performed to study the morphology using FEI Quanta 650 model device (Hillsboro, OR, USA), the Fourier transfer infrared (FTIR) spectrum was used to examine the nature of the chemical bonds by JASCO FT/IR-4600 type device (Tokyo, Japan), Energy dispersive X-ray spectroscopy (EDX) analysis was conducted to know the elemental composition by BRUKER X/6/10 model instrument (Billerica, MA 01821, USA), Thermo-gravimetric analysis (TGA) was performed to study the thermal stability by TGAQ50 module device from Thermal Analyzes device (Borkene, Germany). Moreover, an identification of the point of zero net charge was carried out according to the method described by Suzana Modesto et al. [29].

pH at the Point of Zero Charge (pH_{pzc})

The pH at the point of zero charge (pH_{pzc}) is a significant parameter in the study of the adsorption phenomena, especially when the electrostatic forces are involved. The pH_{pzc} is a relevant indicator of the chemical and electronic properties of the material used as absorbent. The method used to measure this parameter is as follows: solutions of 50 mL of NaCl (0.01 M) were poured into closed flasks and the initial pH (pH_i) was adjusted in each volume, ranging from 2 to 12, by adding different volumes of NaOH or HCl 0.1 M solutions. In each flask, 0.15 g of bio-adsorbent (ALP)was added. After 78 h of storage at room temperature (25 ± 2 °C), the final pH (pH_f) was measured from each solution. On a graph $pH_f = f(pH_i)$, the intersection of the pH curve with the bisector of the first quadrant axis resulted in the pH_{pzc} value [30].

Iodine Number

The iodine number (Id) is used to quantify the porosity of adsorbents, and it is defined as the amount of iodine adsorbed by 1 g of adsorbent.

According to the literature [31], two tests were carried out. The first test is the blank test conducted with 10 mL of a 0.1 N iodine solution, filling a beaker and dosing with a 0.1 N solution of sodium thiosulfate (Na_2SO_3), as long as the color due to a few drops of a starch solution (indicator) vanishes. The second test consists of adding 0.2 g of bio-sorbent, i.e., ALP, to a beaker which contains 15 mL of a 0.1 N iodine solution and mixing it for 4 min with stirring equipment. After that time, a centrifugation process is carried out, and 10 mL of the filtrate (which contains iodine) is dosed with a 0.1 N solution of sodium thiosulfate (Na_2SO_3), as long as the color due to a few drops of a starch solution (indicator) vanishes [32].

The iodine number can be calculated by the following Equation (1):

$$\mathrm{Id} = \frac{[(V_B - V_S) \times \mathrm{N} \times 126.9 \times {}^{15}/_{10}]}{\mathrm{m}} \quad (1)$$

where:

- $(V_B - V_S)$ is the difference between titration volumes calculated for blank test and test with bio-sorbent. Such difference is measured in ml of sodium thiosulfate (0.1 N) solution;
- N is the normality of the sodium thiosulfate solution (0.1 N);
- 126.9 is the atomic mass of iodine, measured in g/mol;
- m is the mass of the bio-adsorbent, measured in g.

Methylene Blue Index

The methylene blue index (in mg/g) is used to quantify the mesopores and macropores constituting the surface of adsorbents. The methylene blue index is measured using the volume, expressed in milliliters, of a standard solution of methylene blue, bleached per 1 g of material.

The method used to measure the concentration of methylene blue is UV-Visible spectroscopy. The methylene blue molecule has actually an adsorption maximum in the light visible range at the wavelength of 664 nm. The measurements were carried out with a Milton Roy Company Spectronic 20D spectrometer (Ivyland, PA, USA). The methylene blue index and, consequently, the adsorption capacity (Q) of artichoke leaves were calculated using the following Equation (2):

$$\mathrm{Q} = \frac{(\mathrm{c_i} - \mathrm{c_e}) \times \mathrm{V}}{\mathrm{m}} \quad (2)$$

where:

- Q is the apparent adsorption capacity (mg/g) of activated carbon related to the adsorbate;
- c_i is the initial concentration (mg/L) of methylene blue solution (20 mg/L)
- c_e is the residual concentration (mg/L) of methylene blue solution (0.855 mg/L)
- V is the volume of methylene blue solution (0.25 L)
- m is the mass (g) of the adsorbent(1 g)

Bio-Adsorbent Surface Analysis

The surface area characterization of ALP was carried out by N_2 adsorption at 77 K using Quantachrome, Nova instrument, by the Brunauer–Emmett–Teller (BET) method. Fourier Transform Infrared spectroscopy (FTIR) is a diagnostic tool for evaluating the nature of the chemical bonds present in molecules: this technique allows for the identification of some important functional groups that have the capacity to adsorb BR dye. The analysis of the BR dye as well as the bio-adsorbent, prior and after use, were performed by infrared spectroscopy using a JASCO FT/IR-4600 type instrument. The scanning electron microscope (SEM) coupled with Energy Dispersive Spectroscopy X-ray (EDX) analysis was carried out for ALP, prior and after the adsorption process. These analyses were conducted

with a FEI Quanta 650/Broker (x/6/10) instrument and identified aspect and morphology of the surface, as well as the elementary composition of materials. The structural characterization of ALP prior and after adsorption was determined by X-ray diffraction analysis (XRD) using a D2 PHASER-BRUKER AXS type device.

2.5. Experimental Design

An experimental design was performed by using Minitab 16.0 software (Minitab, LLC, State College, Pennsylvania, USA) according to a full factorial design (2^k) with k = 3 factors, i.e., pH, temperature and bio-adsorbent dosage, respectively. The effects were studied as related to the removal efficiency of the BR dye.

As shown in Table 1, a range between maximum and minimum values for all factors were set. In addition, the coded and actual values at the two levels (low and high) for 8 optimization experiments are reported in Table 2.

Table 1. Factors' range.

Parameters	Minimum Value	Maximum Value
pH	4	10
Bio-adsorbent dosage (g)	0.5	2
Temperature (°C)	24	80

Table 2. Values of factors for each experience.

Tests	pH (X_1)	Bio-Adsorbent Dosage (g) (X_2)	Temperature (°C) (X_3)
1	4	0.5	24
2	10	0.5	24
3	4	2	24
4	10	2	24
5	4	0.5	80
6	10	0.5	80
7	4	2	80
8	10	2	80

2.6. Mathematical Model Design

The effects and the mutual interaction between different factors were analyzed by using the full factorial design. The mathematical model was carried out on the basis of a linear response function, expressed by the following Equation (3):

$$Y = a_0 + a_1 \times X_1 + a_2 \times X_2 + a_3 \times X_3 + a_{12} \times (X_1 \times X_2) + a_{13} \times (X_1 \times X_3) + a_{23} \times (X_2 \times X_3) + \varepsilon \quad (3)$$

where:

- Y is the response of the experiment, i.e., removal efficiency (R %);
- X_1, X_2, X_3 are the different factors investigated. (X_1 = pH; X_2 = bio-sorbent dose; X_3 = Temperature);
- $a_1, \ldots, a_{23}$ are the effects of factors (coefficients).
- ε is the error of the model.

2.7. Experimental Protocol of Kinetic and Isotherm Adsorption

All the experiments aimed at finding kinetics and isotherms of adsorption of BR on the adsorbent ALP were carried out under static conditions: (i) room temperature of 25 ± 2 °C; (ii) an amount of 1 g of bio-adsorbent (ALP) placed into 250 mL batch reactor; (iii) 250 mL of a solution BR dye-at concentration ranging from 4 mg/L to 100 mg/L added to the solution in each batch reactor. The heterogeneous mixture was stirred for a time ranging between 5 and 180 min. Batch reactors were wrapped in aluminum foil to prevent dye decomposition due to the light. Samples collected from each batch reactor were centrifuged

using a centrifuge at 3500 rpm to separate the liquid phase from the solid (adsorbent and adsorbate, respectively). The liquid phase was analyzed by UV-Visible spectrophotometer to measure the residual dye concentration. The optimal absorption wavelength of BR dye is 549 nm.

The adsorption efficiency was evaluated by calculating Q according to Equation (2), whereas the removal efficiency was calculated using the following Equation (4):

$$R = \frac{(c_0 - c_e)}{c_0} \times 100 \quad (4)$$

where:

- c_0 is the initial concentration of the BR dyes (mg/L);
- c_e is the residual concentration of BR dye at equilibrium (mg/L);

2.8. Thermodynamic Study

The effects of temperature on the adsorption process were studied by varying this parameter from 24 to 80 °C. Tests were carried out by adding 1 g of the ALP to 250 mL of the BR solution at 20 mg/L.

The thermodynamic study assesses the feasibility and spontaneous occurrence of the adsorption process. Parameters such as free energy (ΔG°), enthalpy variation (ΔH°) and entropy variation (ΔS°) can be estimated from the equilibrium constants at different temperatures. ΔG° of the adsorption reaction is calculated by Equation (5):

$$\Delta G^\circ = -R \times T \times \ln(K_{ads}) \quad (5)$$

where:

- K_{ads} is theequilibrium constant;
- ΔG° is the free energy variation (kJ/mol);
- R is the perfect gas constant (8.314 J/(mol·K$^-$)
- T is the absolute temperature (K);
- ΔH° and ΔS° are calculated by Van't Hoff Equation (6) as follows:

$$\ln(K_{ads}) = -\frac{\Delta H^\circ}{RT} + \frac{\Delta S^\circ}{R} \quad (6)$$

3. Results and Discussions

3.1. Bio-Adsorbent Characterization

3.1.1. BET Surface Area Analysis

The results obtained show that the specific surface area (S_{BET}), pore volume (Vp) and pore diameter (pd) were 997.816 m^2/g, 27.148 cm^3/g and 149.875 A°, respectively. These results affect the removal efficiency of BR dye.

3.1.2. FTIR Analysis

The results of FTIR spectra obtained are shown in Figure 1. The weak band at 3273 cm^{-1} represents the vibrations of elongation of O–H groups (e.g., carboxyl, phenols or alcohols) or linked (bound) to amine groups (NH)(the width of the peak indicates an H bond) [33,34].

While the band at 2923 cm^{-1} is characterized by the asymmetric and symmetric stretching vibration of the $–CH_3$ or $–CH_2$ aliphatic groups [35]. The bands at 1744 cm^{-1} and 1611 cm^{-1} are referred to the C=O stretching vibration of the carbonyl group (aldehyde or ester) as well as the symmetrical stretching vibration of the C=C bond, respectively.

The bands of 1415 to 1252 cm^{-1} are due to the C–O elongation vibration and confirm the presence of carboxyl/alcohol/ether/ester functional groups in the molecular composition of the bio-absorbent. The presence of fluorinated aliphatic compounds (C–F) or C–N

bonds is likely in the region around 1015 cm^{-1} of the FTIR spectrum of ALP [36]. The wide band at 523 cm^{-1} could be due to the –C–H bending vibration of the alkene [37].

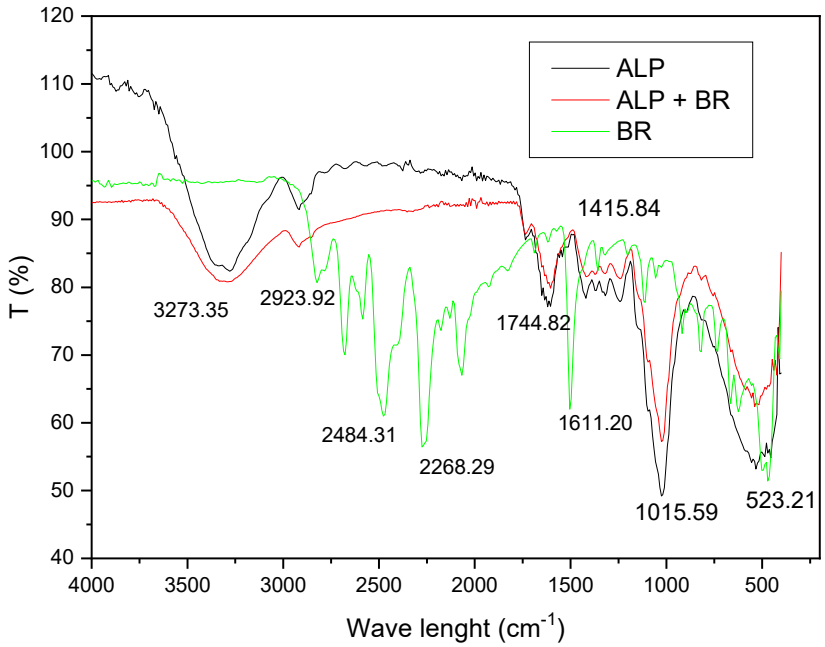

Figure 1. FTIR spectra of BR, ALP and ALP + BR.

The comparison between the two spectra (the raw ALP and the ALP adsorbing BR) shows a decrease of intensity in the range 2000–500 cm^{-1}, for ALP + BR. This result is a consequence of the adsorption of dye onto the adsorbent surface, thus reducing the amount of –C–H– functional groups [33]. Observing Figure 1, spectra of the exhausted bio-sorbent differs from that of the raw bio-sorbent for those wave lengths where the differences between BR dye and raw ALP are more evident (i.e., from 4000 to 1800 cm^{-1}), thus confirming the adsorption of BR onto ALP.

3.1.3. SEM Analysis

Figure 2 shows the surface morphology of raw ALP examined by scanning electronic microscopy (SEM)with different magnifications (a: 5 μm), (b: 20 μm), (c: 50 μm) and (d: 400 μm). This image shows that the pores of the ALP are highly heterogeneous with large pore size: this specific aspect is favorable for the absorption of BR dye molecules. Figure 3 shows the surface morphology of ALP combined with BR after Bengal Rose dye adsorption, examined by scanning electronic microscopy (SEM)with different magnifications (a: 5 μm), (b: 20 μm), (c: 50 μm) and (d: 400 μm).

3.1.4. Energy Dispersive Spectroscopy (EDX)

Figures 4 and 5 report the results obtained from energy dispersive spectroscopy (EDX) analysis for raw ALP and ALP combined with BR, after adsorption. This analysis is carried out mainly to determine the elemental composition of the ALP bio-adsorbent in its raw state and after adsorption (ALP + BR). The result shows that carbon and oxygen are the main constituents for the two states of ALP, raw and combined with BR (ALP + BR), after adsorption, thus confirming the organic and acidic nature of the bio-adsorbent [38]. In more detail, ALP after the adsorption of BR dye contains greater C and O content due to the structure of the dye, which is rich in both elements. On the other hand, a significant amount of N and a small amount of Fe and Mg were observed in the raw bio-absorbent, whereas, after use, none of these elements were found. Moreover, no amount of S was detected in the raw bio-adsorbent, whereas a trace of S was present in the exhausted bio-adsorbent.

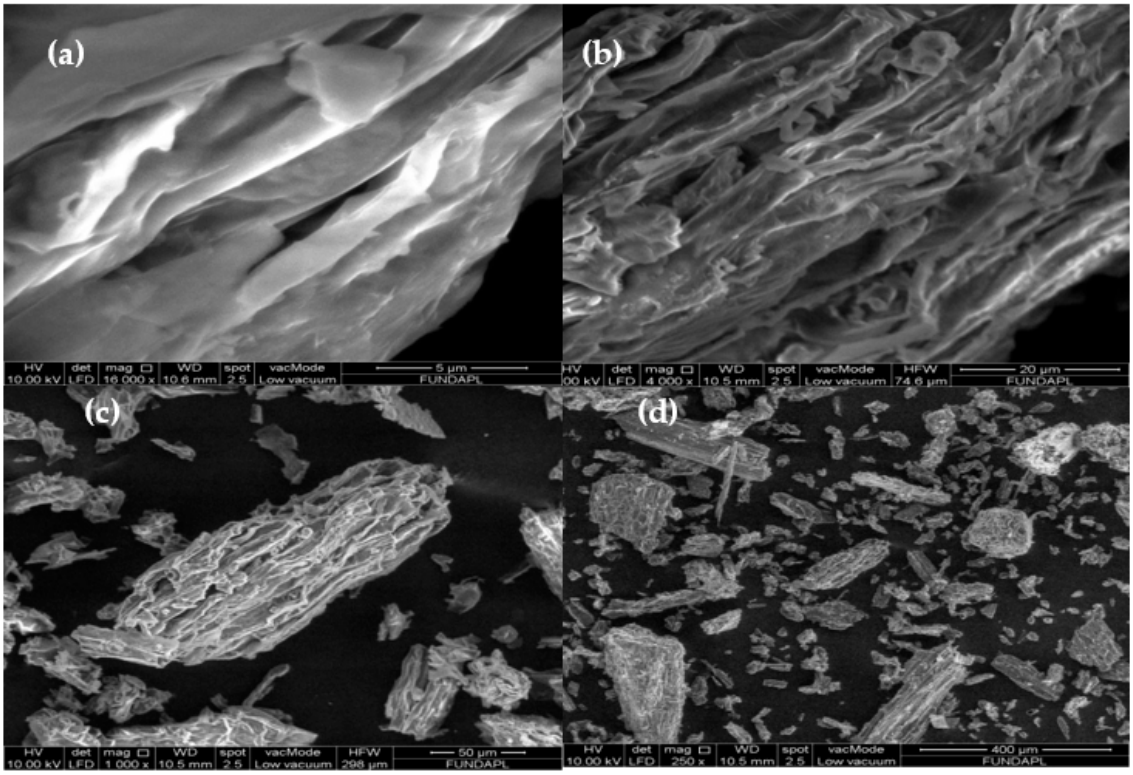

Figure 2. SEM of ALP prior adsorption with different magnifications ((**a**): 5 µm), ((**b**): 20 µm), ((**c**): 50 µm) and ((**d**): 400 µm).

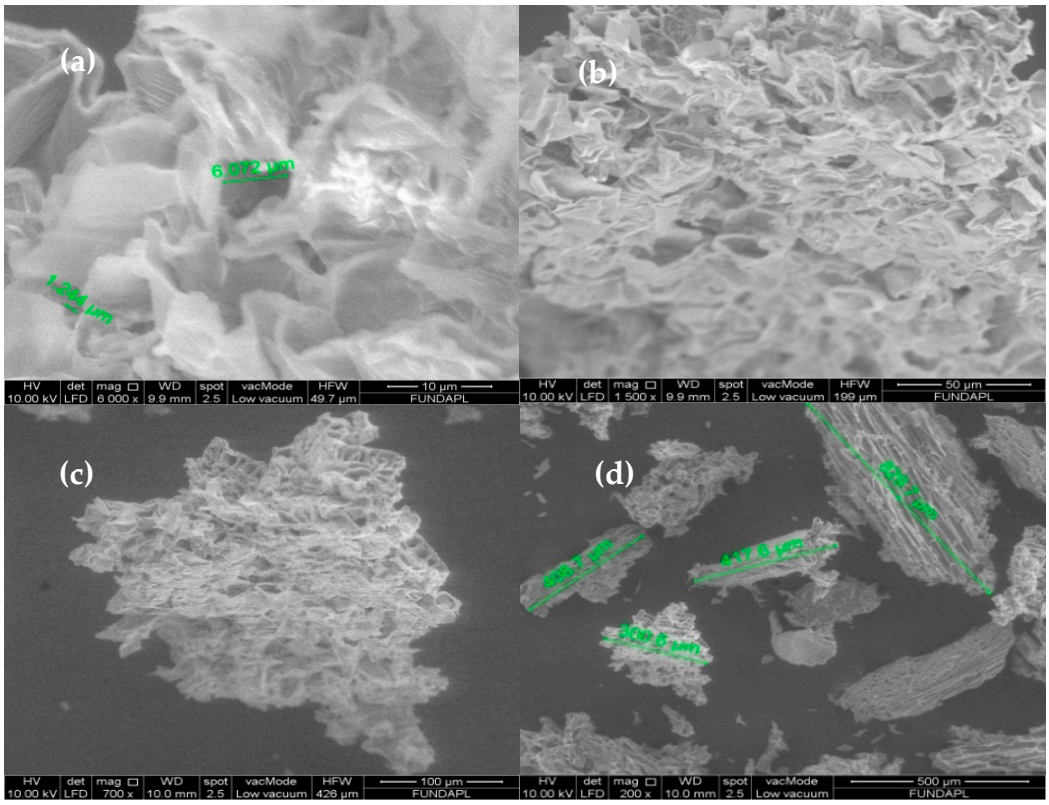

Figure 3. SEM of ALP after adsorption with different magnifications ((**a**): 5 µm), ((**b**): 20 µm), ((**c**): 50 µm) and ((**d**): 400 µm).

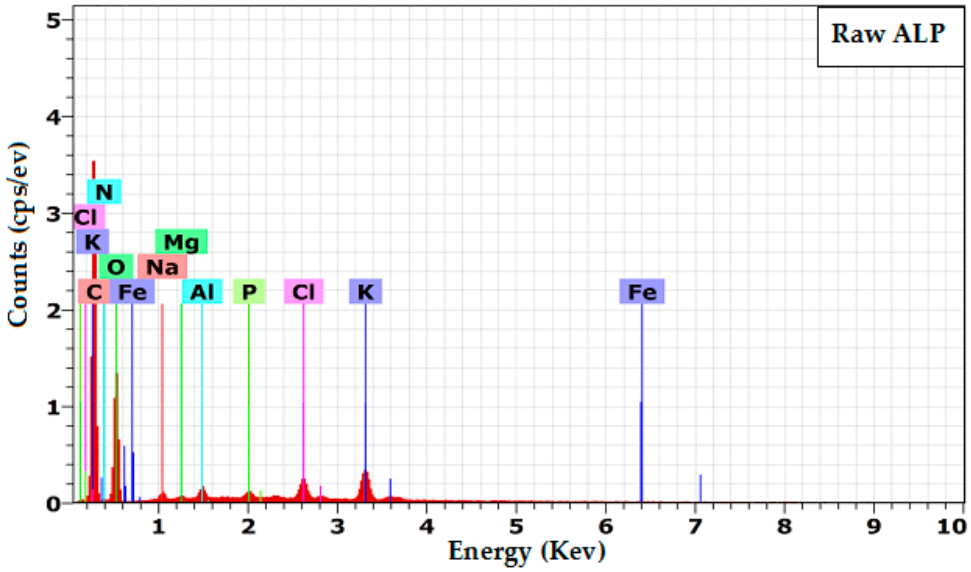

Figure 4. Energy Dispersive Spectroscopy (EDX) for raw material.

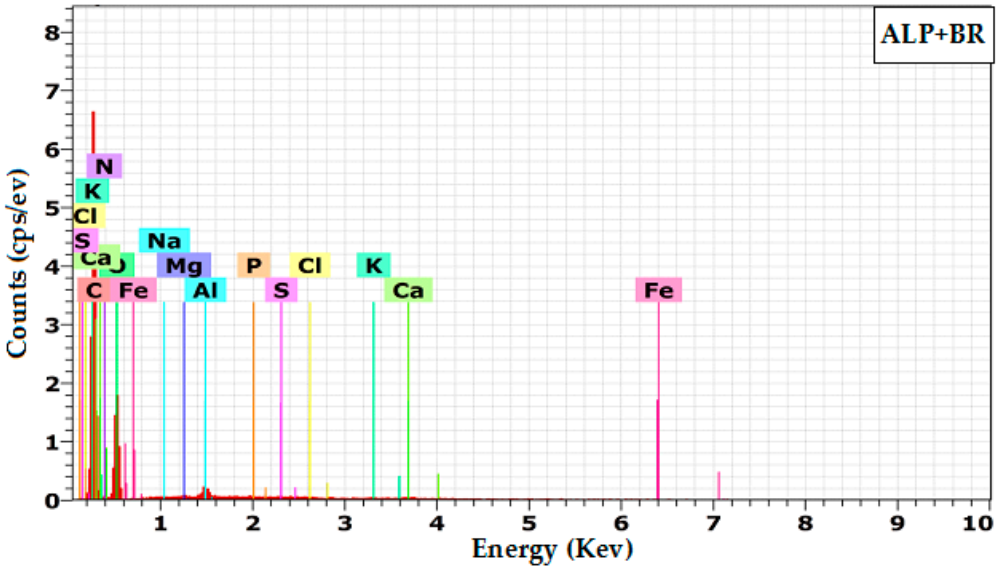

Figure 5. Energy Dispersive Spectroscopy (EDX) after adsorption.

3.1.5. X-ray Analysis

The diffractogram of the raw ALP in Figure 6 does not show the horizontal baseline, thus proving that the material of the bio-adsorbent is amorphous. However, some peaks of the curve emerging from the baseline indicate the presence of a small quantity of crystalline material. Peaks ranging between 10° and 23° correspond to the specific peaks of cellulose and hemi-cellulose [39], therefore, the presence of these diffraction peaks indicates that the biomaterial is semi-crystalline, and according to the work of Jianxin He et al. [40], the peak of $2\theta = 22°$ indicates cellulose of monoclinic structure.

3.1.6. Thermo Gravimetric Analysis

The thermogravimetric analysis (TGA) of raw ALP is shown in Figure 7. The curve is characterized by four steps of thermal degradation. The first step, from 25 to 100 °C, is a dehydration phase, characterized by a mass loss of 8.55%. This loss is due to the water content of the bio-adsorbent. The second step, from 100 to 220 °C, concerns the decomposition of organic components, and is characterized by a mass loss of 16.52%, likely

due to amine group ($-NH_2$) volatilization [41]. The third step, from 220 to 322 °C, shows a remarkable mass loss of 58.7% in 10 min. This mass loss indicates the decomposition of the main constituents of the biomaterial. The last step, from 322 to 900 °C, amounts to a weight loss of 92.6% caused by the cracking of the phenyl group as well as the loss of the hydrocarbon parts [42]. Finally, the first step, from 25 to 220 °C, is due to the water (moisture). The second stage is due to the degradation of hemi-cellulose and cellulose, while the third stage is due to the decomposition of residual lignin [43]. A similar result is present in the international literature; a TGA analysis for artichoke leaves during a pyrolysis process showed five decomposition steps with a total weight loss of 81.8% [44].

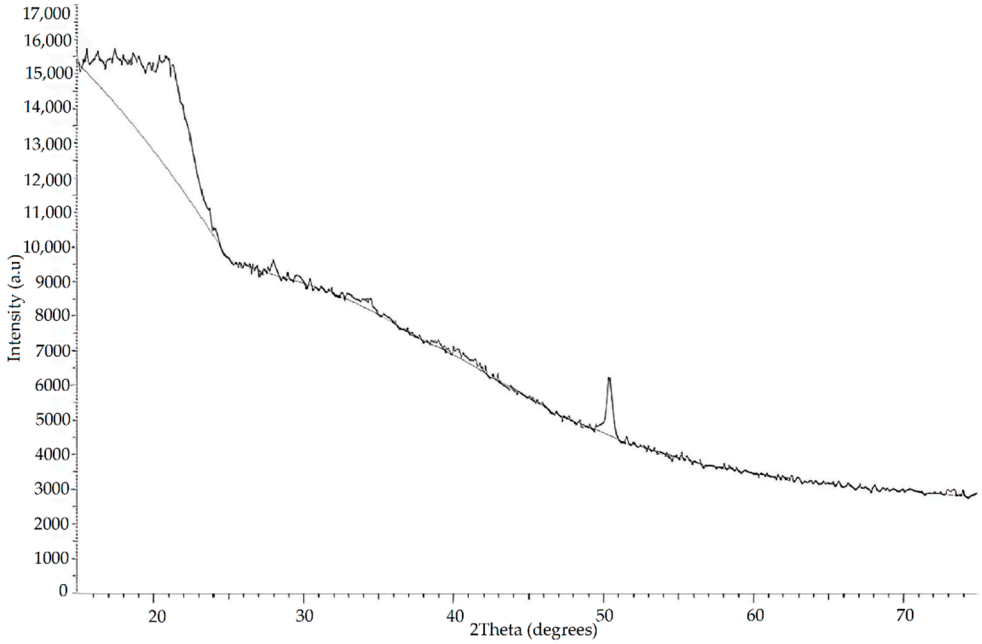

Figure 6. X-ray analysis of artichoke leave powder.

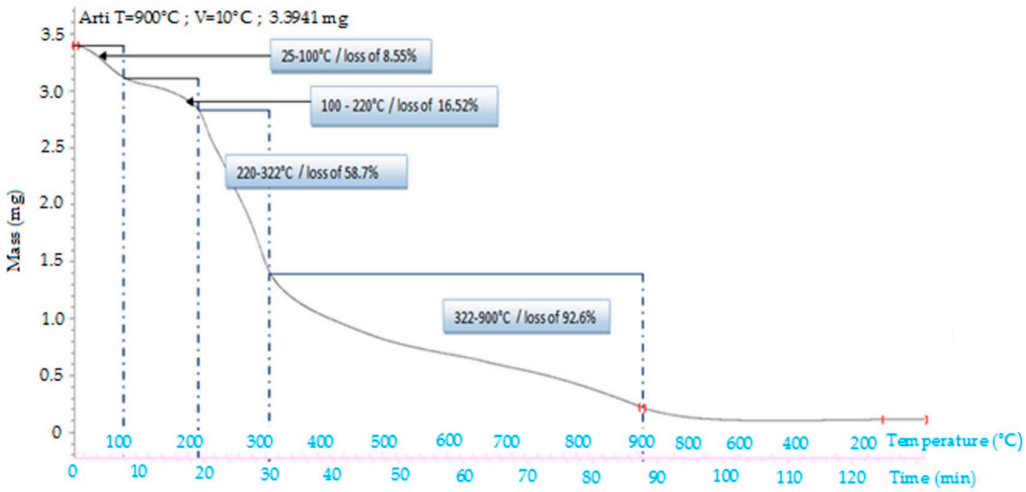

Figure 7. Thermo Gravimetric Analysis (TGA) of raw artichoke leaves powder (ALP).

3.1.7. The pH Zero Charge Point (pH_{pzc})

Figure 8 reports the graphical value of pH_{pzc}. At pH = 4.3 the surface charge is zero (neutral surface). For pH values higher than pH_{pzc} the bio-sorbent surface charge is negative. Otherwise, if the pH of the solution is lower than the pH_{pzc}, the surface of the material is positively charged.

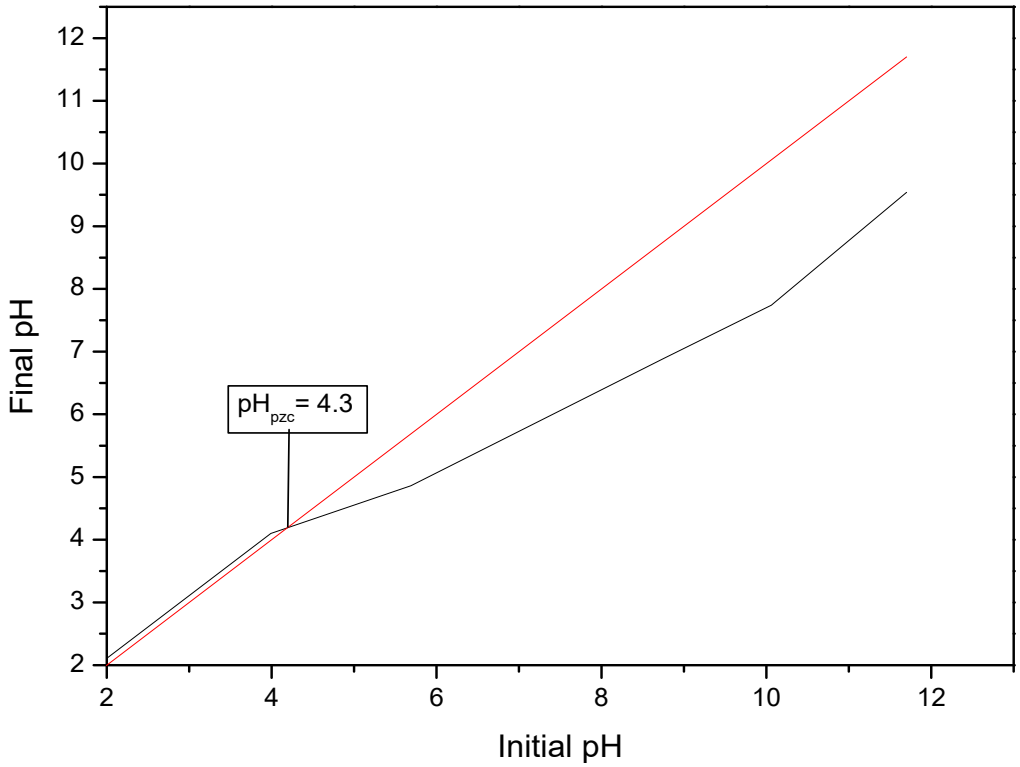

Figure 8. pH value of the point of zero charge (pH_{pzc}) for raw ALP bio-sorbent.

In all the experiments, the pH of solutions were maintained constantly equal to 4, therefore, the surface of bio-sorbent (ALP) can be considered positively charged. ($pH_{solution} < pH_{pzc}$).

3.1.8. Iodine and Methylene Blue Index

The iodine test was used to assess the presence of appropriate micro-porosity for the adsorption of dyes [44]. The value obtained, according to Equation (1), is as follows:

$$Id = 323.595 \text{ mg/g}$$

This result proves that the bio-adsorbent surface is characterized by micro-porousness, as the iodine retention capacity is significantly high.

The results obtained from methylene blue index tests, are shown in Table 3.

Table 3. Methylene blue adsorption capacity.

Time (min)	5	10	30	60	90	120
absorbance (664 nm)	0.3279	0.2975	0.2961	0.1758	0.1782	0.201
Q (mg/g) (v = 250 mL)	4.60	4.64	4.64	4.79	4.78	4.75
R (%)	92.02	92.76	92.79	95.72	95.66	95.11

Data in Table 3 show that the bio-adsorbent retains methylene blue significantly well after 60 min of contact time. The maximum adsorption efficiency was 95.72%.

The methylene blue index (MBI) is equal to 4.79 mg/g.

This value shows that 1 g of bio-adsorbent can adsorb 4.79 mg of methylene blue, proving that the bio-adsorbent presents a low macro-porosity.

3.2. Factorial Design

The results from the modeling experimental design are reported in Table 4. Table 4 shows that the highest removal efficiency of 86.5% was obtained for the following optimal conditions: pH = 4, T = 80 °C and bio-adsorbent dosage of 8 g/L.

Table 4. Results of factorial design in terms of capacity and removal efficiency of BR dye onto ALP.

pH	Mass (g)	Temperature (°C)	Q (mg/g)	Efficiency (%)
4	0.5	24	7.42	68.46
10	0.5	24	2.84	26.24
4	2	24	1.35	50.11
10	2	24	1.59	58.6
4	0.5	80	8.11	74.8
10	0.5	80	0.64	5.95
4	2	80	2.34	86.5
10	2	80	1.88	69.66

From Figure 9, it can be noticed that the pH has a negative effect on the response (removal efficiency of adsorption process), thus showing a decrease in the removal efficiency by 75% at low value of pH (4) and 40% at high value of pH (10). On the other hand, the dosage of ALP has a positive effect ranging from an increase of efficiency by 45% (−1) up to 65% (+1). Temperature showed a negligible effect. Therefore, the removal efficiency of BR dye reached the highest performance in acidic condition.

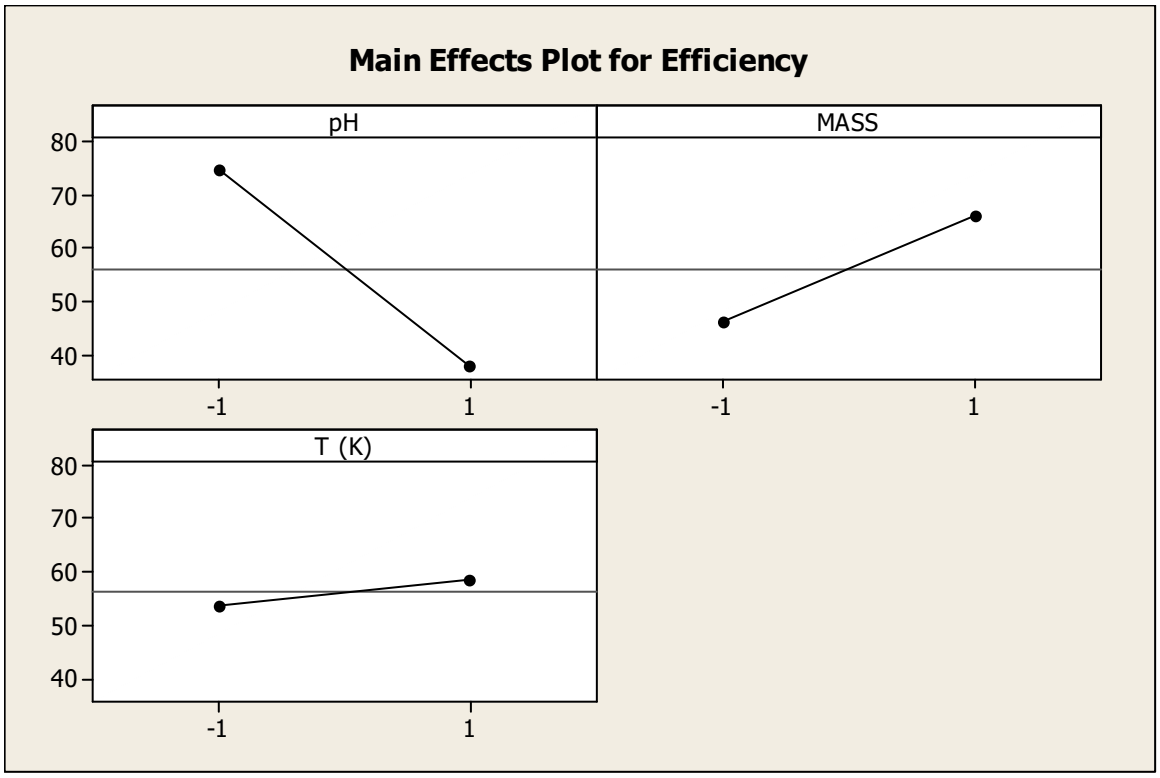

Figure 9. Effect of the investigated factors on BR dye removal efficiency.

Figure 10 shows that the interactions with the greatest effects are due to pH and mass as well as to mass and temperature. On the other hand, the interaction of pH with temperature resulted in a negligible effect.

According to Minitab software, the optimum response of the highest removal efficiency (88.2%) was obtained for the following parameters' values: mass = 2 g, pH = 4 and T = 80 °C, with a correlation coefficient R^2 = 88.2 and desirability D = 0.98 (Figure 11).

Finally, the residual error (ε) between the model response and the experimental values was equal to 2.45 (88.2 − 85.75 = 2.45).

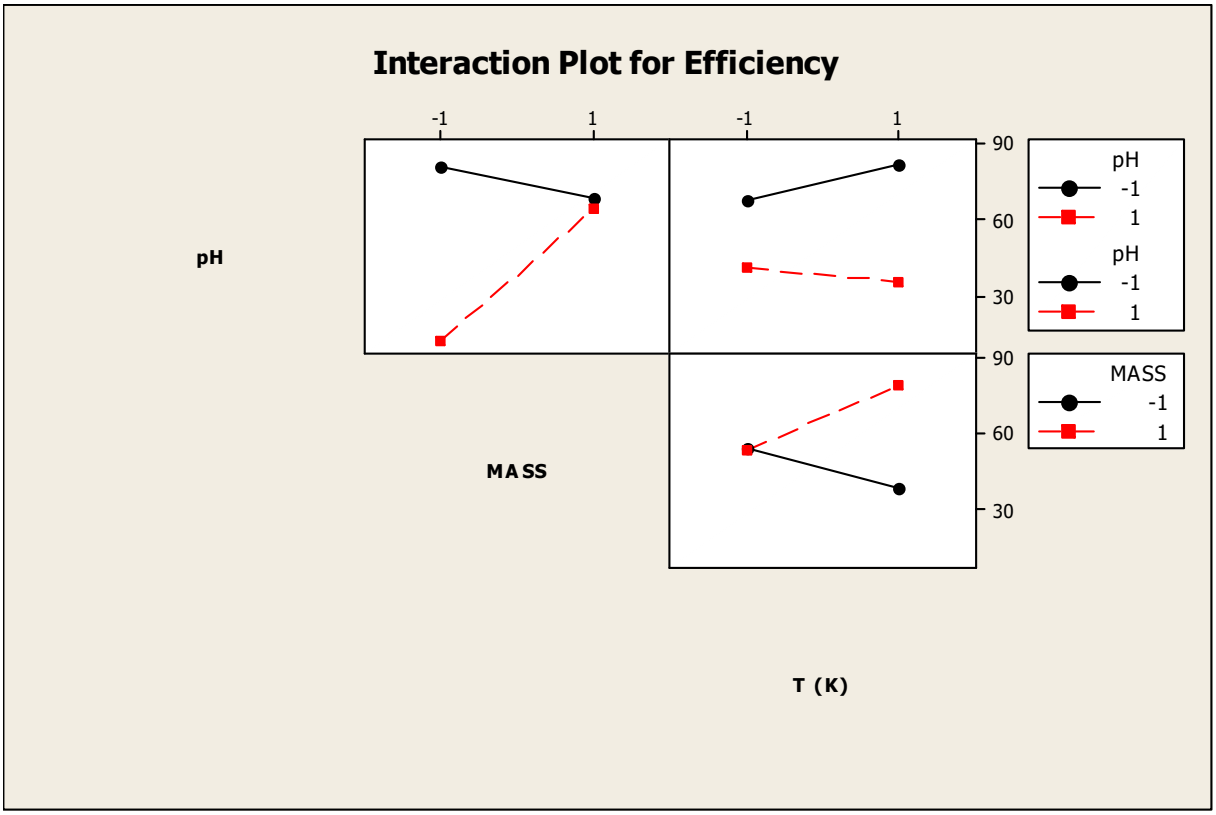

Figure 10. Effects of mutual interactions among factors on BR dye removal efficiency.

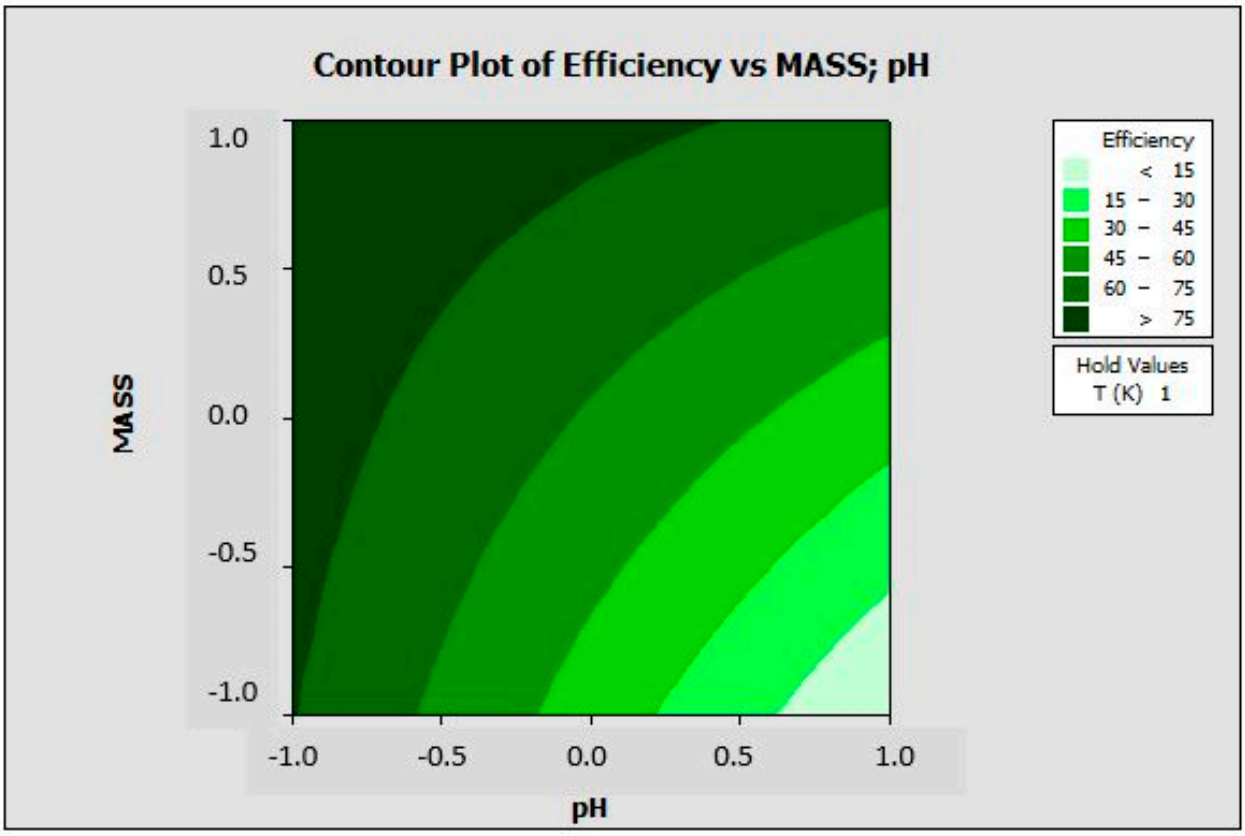

Figure 11. Contour plot of variation of efficiency as a function of mass and pH at T = 80 °C.

The factorial design study resulted in the following empirical Equation (7) where the removal efficiency (Y) of BR dye by ALP is expressed as a function of the sole affecting factors:

$$Y = 6.18 - 18.34 \times pH + 9.99 \times M + 2.40 \times T + 16.08 \times pH \times M - 4.92 \times pH \times T + 10.46 \times M \times T + 2.4 \quad (7)$$

3.3. Parametric Study of the Adsorption of BR Dye onto the ALP Surface

3.3.1. Effect of Contact Time

From Figure 12, it can be noticed that the removal of BR dye by ALP begins instantaneously. According to Figure 2, the initial high adsorption rate is a consequence of the pore emptiness. The progressive filling of pores is responsible for a reduction of the adsorption capacity and the achievement of equilibrium condition after 40 min. The adsorption capacity of BR dye by ALP was 4.07 mg/g, which corresponds to a BR dye removal efficiency of 80.1%.

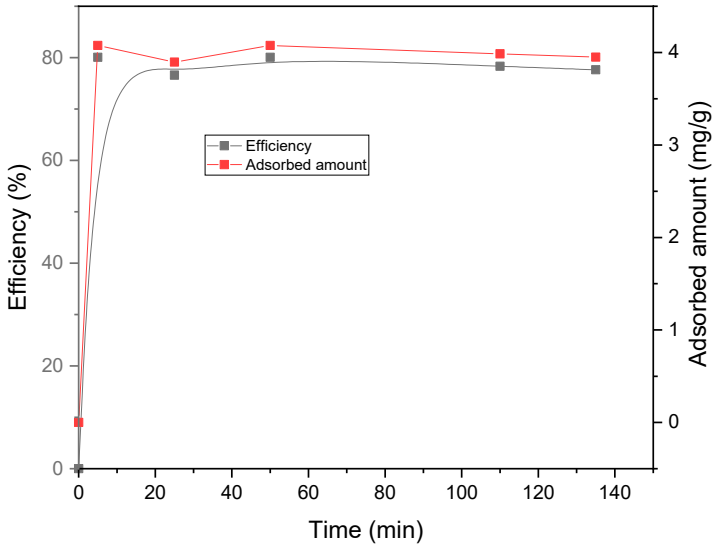

Figure 12. Trend of BR dye adsorption onto ALP.

3.3.2. Effect of Temperature

The curves of adsorption efficiency for the two target temperatures are reported in Figure 13. This figure shows that the highest adsorption capacity was reached after 45 min and amounted to 4.2 mg/g, with a removal efficiency of 87.46% at the temperature of 80 °C. At 24 °C, the performance was less, since after 45 min, an adsorption capacity of 3.0 mg/g and a removal efficiency of 60.7% were achieved.

3.3.3. Effect of Initial Concentration of RB Dye

Figure 14 shows the effect of initial BR dye concentration on the adsorption process. The figure shows that the adsorbed amount (capacity Q) of BR dye increases with the increase of its initial concentration in the contaminated solution. Figure 14 shows that, when the initial concentration is set equal to $C_{0\,BR}$ = 100 mg/L, the adsorption capacity is almost fourfold that obtained with $C_{0\,BR}$ = 20 mg/L. This result can be explained by the presence of a strong gradient of BR dye concentration between the solution and the surface of the adsorbent.

3.4. Kinetics Study of the Adsorption of BR Dye by ALP

To determine the order of the adsorption kinetic and to explore the adsorption mechanism for the adsorption system (BR/ALP), the pseudo-first-order, pseudo-second-order and intra-particle diffusion kinetic models were tested.

The values of the constants of the different kinetic models for the adsorption of BR by ALP for the studied system are grouped in Table 5. The results show that the correlation coefficients R^2 for the linear plots of the pseudo-second-order equation were close to 1, with a value of 0.999 for all the investigated concentrations.

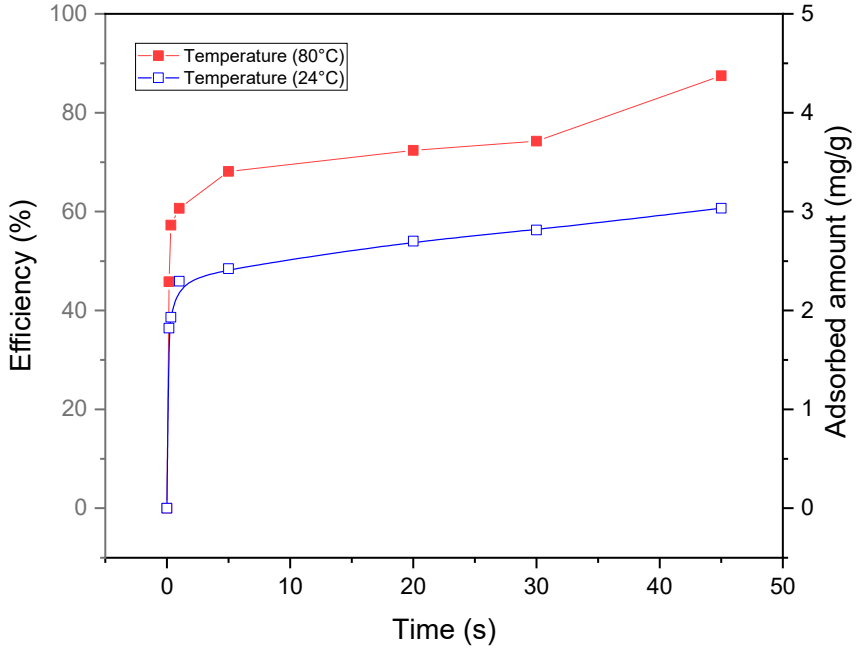

Figure 13. Effect of temperature on BR dye adsorption.

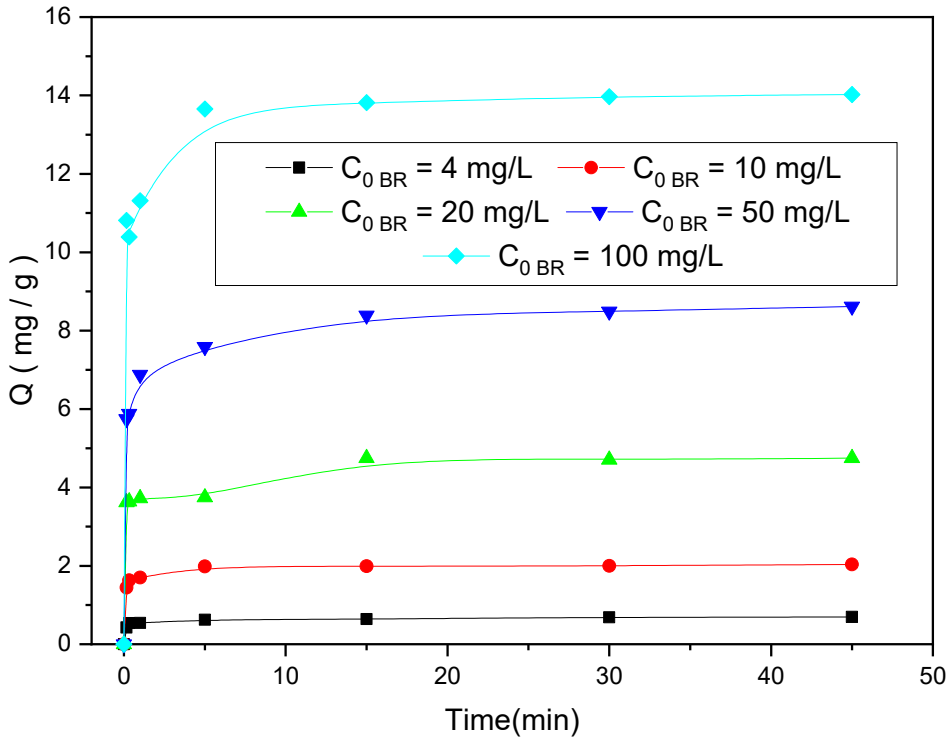

Figure 14. Effect of the initial concentration on the adsorption of BR dye.

The adsorbed quantity calculated by the pseudo second order equation is close to the experimental adsorbed quantity. For example, at 20 mg/L qe, cal (BR/ALP) was equal to 4.29 mg/g and qe, exp(BR/ALP) equal to 4.07 mg/g, whereas at 100 mg/L qe, cal (BR/ALP)

was equal to 14.06 mg/g and qe, exp(BR/AL)was equal to 14.84 mg/g, thus confirming that the pseudo-second-order model is the most applicable in the case of discoloration of BR in the studied system. The results suggested that the dye uptake process is attributed to chemical adsorption, even though physical adsorption and chemical adsorption may be difficult to distinguish [45].

Table 5. Kinetic parameters for the adsorption of BR dye onto ALP.

	Pseudo First-Order Kinetic $\ln(q_e - q_t) = \ln q_e - \frac{K_1}{2.303} t$			**Pseudo Second-Order Kinetic** $\frac{t}{q} = \frac{1}{K_2 \cdot q_e^2} + \frac{1}{q_e} t$			**Intra Particle Diffusion Model** $q_t = K_{in} \times t^{1/2}$	
C_0 (mg·L^{-1})	R^2	K_1 (min^{-1})	q_e (mg/g)	R^2	K_2 (g·mg^{-1}·min^{-1})	q_e (mg/g)	R^2	K_{int} (mg·g^{-1}·min$^{-1/2}$)
4	0.8132	0.103	4.17	0.9994	3.4	0.96	0.801	0.0344
10	0.5743	0.1038	2.32	0.9999	2.9897	2.03	0.7039	0.0778
20	0.761	0.1756	1.15	0.9999	0.5377	4.29	0.8922	0.0601
50	0.8289	0.1194	2.85	1	0.4513	8.63	0.8444	0.4482
100	0.8018	0.155	3.39	0.9998	0.3575	14.06	0.7527	0.7527

3.5. Adsorption Isotherm

The adsorption isotherms are often used to assess the maximum pollutant fixation's capacity and to identify the types of adsorption. The adsorption isotherm of BR onto ALP is shown in Figure 15, where the variation of the adsorption capacity is represented as a function of the equilibrium concentrations.

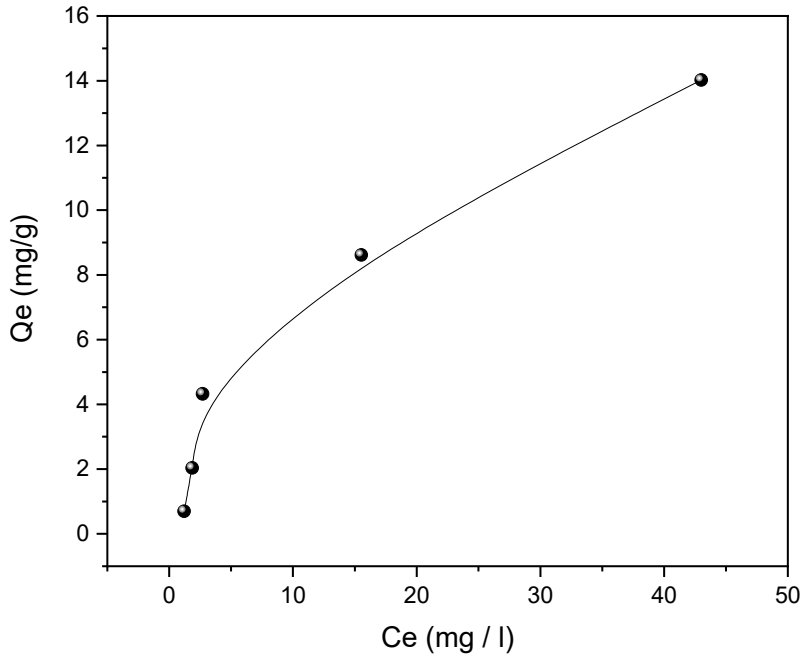

Figure 15. Adsorption isotherm of BR on to ALP.

The resulting isotherm constant parameters for the adsorption of BR onto ALP according to Langmuir, Freundlich, Temkin and Elovich linear models are reported in Table 6.

The shape of the curve in the Figure 15, i.e., type "L", shows a progressive monolayer saturation of the biomaterial.

The results in Table 6 show that the value of the Temkin's and the Freundlich's correlation coefficients (R^2) are the highest values for all studied systems, but that of Langmuir is not too far from the unit. However, for the Langmuir isotherm, the adsorbed quantity calculated by this model (11.11 mg/g) is different from the experimental adsorbed quantity (about 14 mg/g), but it was very close to the value obtained with the Temkin model (13.3 mg/g).

Table 6. Isotherm constant parameters for the adsorption of BR onto ALP.

Type of Isotherm	Linearization of Equations	Constants	R^2
Langmuir	$\frac{1}{q_e} = \frac{1}{q_{max}} + \frac{1}{K_L \times C_e \times q_{max}}$	q_{max} = 11.11 (mg/g) K_L = 0.058 (L/mg)	0.912
Freundlich	$\ln(q) = \ln(K_f) - \frac{1}{n} \times \ln(C_e)$	K_f = 1.13 $(mg \cdot g^{-1} \cdot (L \cdot mg^{-1})^{1/n})$ 1/n = 0.725	0.92
Temkin	$q_e = \frac{RT}{b_T} \times \ln(A_T) + \frac{RT}{b_T} \times \ln(C_e)$	RT/b_T = 3.52 $\ln(A_{T)}$ = 0.074	0.98
Elovich	$\ln\left(\frac{q_e}{C_e}\right) = \ln(K_E \times q_m) - \frac{q_e}{q_m}$	q_m = 13.3 (mg/g) K_E = 0.083	0.65

Where:

- q_e and q_{max} are the equilibrium and maximum capacity of adsorption (mg/g);
- C_e is the equilibrium concentration of BR (mg/L);
- K_L, K_f, K_E are the Langmuir, Freundlich and Elovich constants, respectively;
- R is the universal gas constant, 8.314 J/(mol·K);
- T is the absolute temperature (K);
- b_T is the change in the adsorption energy (J/mole)
- A_T is the Temkin constant (L/mg)

The separation factor (R_L) of the Langmuir isotherm can be defined by Equation (8). The value of R_L indicates whether the adsorption process is irreversible (R_L = 0), favorable (0 < R_L < 1), linear (R_L = 1),or unfavorable (R_L > 1) [46].

$$R_L = \frac{1}{1 + (K_L \times C_0)} \quad (8)$$

The R_L value ranges between 0.147 and 0.812 for BR at the different initial concentrations (4–10–20–50–100 mg/L). This result proves the favorable adsorption of BR dye onto ALP [47].

3.6. Thermodynamic Study

In order to describe the thermodynamic behavior of BR bio-sorption onto ALP from aqueous solutions, the thermodynamic parameters including change in free energy (ΔG°), enthalpy (ΔH°) and entropy (ΔS°), were calculated. Figure 16 shows the linear variation of $\ln(K_{ads})$ as a function of (1/T). This curve has a slope, i.e.,ΔH°/R and Y-intercept, i.e., ΔS°/R. The adsorption thermodynamic parameters were determined from the experimental results obtained at different temperatures (Figure 16).

Table 7 shows that the value of ΔH° was negative, thus confirming the exothermic nature of the adsorption reaction that is responsible for a decrease in the adsorbed amount of BR onto ALP when the temperature increases. Regarding ΔS°, this parameter shows a negative value as well, and proves the decrease in randomness at the solid-solution interface. In contrast, the positive value of ΔG° indicates that the BR adsorption process onto ALP was spontaneous. It can be also noticed that ΔG° increases with the increase of the temperature of the solution for all the experiments, thus confirming that the adsorption process is very difficult and disadvantaged when the temperature is very high. Moreover, during the adsorption, the random appearance increases at the solid-solution interface. This phenomenon can be explained by the redistribution of energy between the adsorbent and the adsorbate [48].

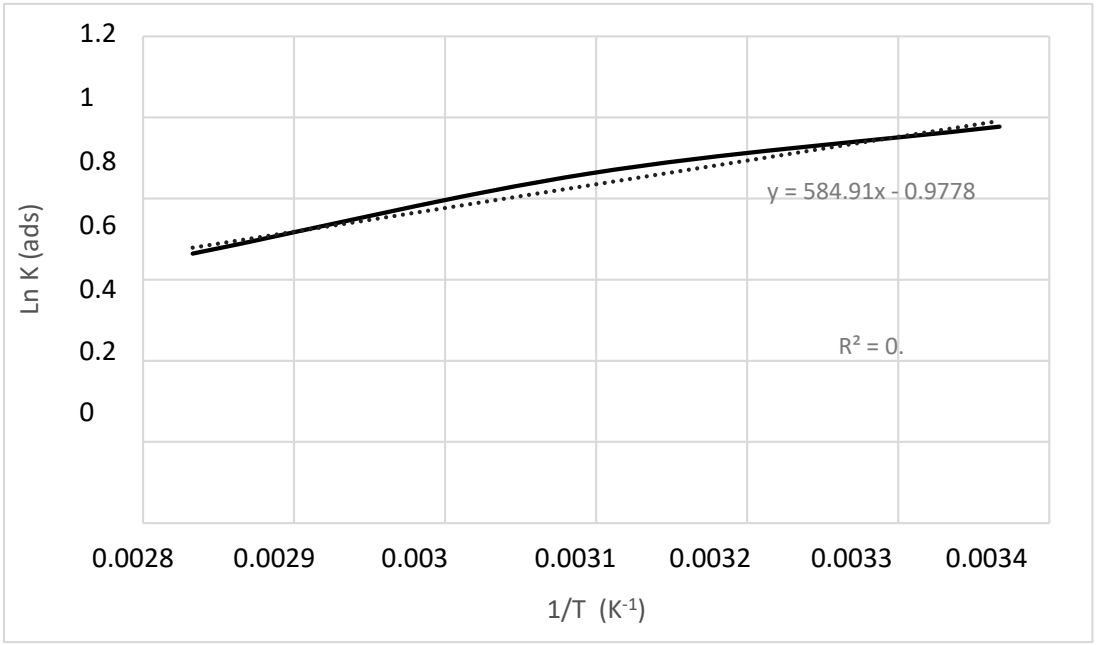

Figure 16. Ln(K_{ads}) as function of 1/T.

Table 7. Thermodynamic parameters for adsorption of BR into ALP.

Parameters	Temperature (K)		
	297	**323**	**353**
ΔG° (kJ/mol)	−2.411	−2.314	−1.948
ΔS° (J/(mol·K)		−8.129	
ΔH° (kJ/mol)		−4.86	
R^2		0.9745	

4. Conclusions

In this paper, a new bio-adsorbent, i.e., ALP, obtained from artichoke leaves, was tested to remove BR dye from a liquid phase. The bio-absorbent was characterized by several methods, such as FTIR spectra, SEM, EDX, iodine number, methylene blue index and pH_{pzc}. The study of the effects of several physicochemical parameters on the BR adsorption process by ALP was carried out, and the experimental results showed that both pH and temperature have important effects on the adsorption process, and the optimal values were pH = 4 and T = 24 °C, respectively.

The experimental data were analyzed using several kinetic models. The results obtained showed that the process is adequately simulated by the pseudo-second-order model. The BR dye adsorption isotherm onto ALP is satisfactorily described by each of Temkin's, Freundlich's and Langmuir's models. On the other hand, the thermodynamic study shows that the reaction of adsorption for the couple BR/ALP is spontaneous and exothermic. A 2^3 factorial design of experiments were used to study the effects of three factors (pH, temperature and bio-adsorbent dosage) on the adsorption capacity related to BR dye. The linear model fit well with the experimental data according to the correlation coefficient R^2 = 88.2 and desirability D = 0.98. Furthermore, the interaction parameters were studied. The statistical analysis of the results obtained shows that the mutual interaction between pH and bio-adsorbent dosage strongly affects the BR dye removal efficiency. Optimal values of pH, bio-adsorbent dosage and temperature were 4; 8 g/L and 80 °C, respectively. The maximum removal efficiency was 88%. Finally, ALP is an inexpensive and easy-to-produce bio-adsorbent with solid–liquid separation, which can be used successfully in the treatment and removal of dyes, such as BR, from industrial wastewater.

Author Contributions: Conceptualization, A.K. (Amel Khalfaoui), K.D., A.P.; methodology, A.K. (Amel Khalfaoui), A.B., G.C., A.P.; formal analysis, A.B., K.D.; investigation, A.K. (Amel Khalfaoui); data curation, M.N.K., A.K. (Anouar Khelfaoui), A.B., K.D., C.G.; writing—original draft preparation, A.K. (Amel Khalfaoui), A.B., M.N.K., A.K. (Anouar Khelfaoui), A.P., A.K. (Anouar Khelfaoui), K.D., G.C., C.G.; supervision, A.K. (Amel Khalfaoui), K.D., A.P., C.G.; project administration, K.D. All authors have read and agreed to the published version of the manuscript.

Funding: This research received no external funding.

Acknowledgments: We warmly thank the University Saad Dahleb of Blida, the National Polytechnic of Constantine and the University of Constantine 3 for their support for the realization of the experimental part as well as the physicochemical analyzes and the characterization of the bi-adsorbent.

Conflicts of Interest: The authors declare that they have no known competing financial interests or personal relationships that could have appeared to influence the work reported in this paper.

References

1. Shindhal, T.; Rakholiya, P.; Varjani, S.; Pandey, A.; Ngo, H.H.; Guo, W.; Ng, H.Y.; Taherzadeh, M.J. A critical review on advances in the practices and perspectives for the treatment of dye industry wastewater. *Bioengineered* **2021**, *12*, 70–87. [CrossRef] [PubMed]
2. Ben Slama, H.; Bouket, A.C.; Pourhassan, Z.; Alenezi, F.N.; Silini, A.; Cherif-Silini, H.; Oszako, T.; Luptakova, L.; Golińska, P.; Belbahri, L. Diversity of synthetic dyes from textile industries, discharge impacts and treatment methods. *Appl. Sci.* **2021**, *11*, 6255. [CrossRef]
3. Pang, Y.L.; Abdullah, A.Z. Current status of textile industry wastewater management and research progress in Malaysia: A review. *Clean Soil Air Water* **2013**, *41*, 751–764. [CrossRef]
4. Gros, M.; Petrović, M.; Ginebreda, A.; Barceló, D. Removal of pharmaceuticals during wastewater treatment and environmental risk assessment using hazard indexes. *Environ. Int.* **2010**, *36*, 15–26. [CrossRef] [PubMed]
5. Geissen, V.; Mol, H.; Klumpp, E.; Umlauf, G.; Nadal, M.; van der Ploeg, M.; van de Zee, S.E.A.T.M.; Ritsema, C.J. Emerging pollutants in the environment: A challenge for water resource management. *Int. Soil Water Conserv. Res.* **2015**, *3*, 57–65. [CrossRef]
6. Chung, K.-T. Azo dyes and human health: A review. *Environ. Sci. Health Care* **2016**, *34*, 233–261. [CrossRef]
7. Ismail, M.; Gul, S.; Khan, M.I.; Khan, M.A.; Asiri, A.M.; Khan, S.B. Green synthesis of zerovalent copper nanoparticles for efficient reduction of toxic azo dyes congo red and methyl orange. *Green Process. Synth.* **2019**, *8*, 135–143. [CrossRef]
8. Malik, A.; Akhtar, R.; Grohmann, E. Environmental deterioration and human health: Natural and anthropogenic determinants. In *Environmental Deterioration and Human Health: Natural and Anthropogenic Determinants*; University Freiburg: Freiburg, Germany, 2014; pp. 1–421. ISBN 9789400778900.
9. Sadri Moghaddam, S.; Alavi Moghaddam, M.R.; Arami, M. Coagulation/flocculation process for dye removal using sludge from water treatment plant: Optimization through response surface methodology. *J. Hazard. Mater.* **2010**, *175*, 651–657. [CrossRef]
10. Liu, M.; Yin, W.; Zhao, T.L.; Yao, Q.Z.; Fu, S.Q.; Zhou, G.T. High-efficient removal of organic dyes from model wastewater using $Mg(OH)_2$-MnO_2 nanocomposite: Synergistic effects of adsorption, precipitation, and photodegradation. *Sep. Purif. Technol.* **2021**, *272*, 118901. [CrossRef]
11. Peng, H.; Guo, J. Removal of chromium from wastewater by membrane filtration, chemical precipitation, ion exchange, adsorption electrocoagulation, electrochemical reduction, electrodialysis, electrodeionization, photocatalysis and nanotechnology: A review. *Environ. Chem. Lett.* **2020**, *18*, 2055–2068. [CrossRef]
12. Ledakowicz, S.; Paździor, K. Recent achievements in dyes removal focused on advanced. *Molecules* **2021**, *26*, 870. [CrossRef] [PubMed]
13. Malek, N.N.A.; Jawad, A.H.; Ismail, K.; Razuan, R.; ALOthman, Z.A. Fly ash modified magnetic chitosan-polyvinyl alcohol blend for reactive orange 16 dye removal: Adsorption parametric optimization. *Int. J. Biol. Macromol.* **2021**, *189*, 464–476. [CrossRef] [PubMed]
14. Hendaoui, K.; Trabelsi-Ayadi, M.; Ayari, F. Optimization and mechanisms analysis of indigo dye removal using continuous electrocoagulation. *Chin. J. Chem. Eng.* **2021**, *29*, 242–252. [CrossRef]
15. Sultana, S.; Khan, M.Z.; Umar, K.; Ahmed, A.S.; Shahadat, M. SnO_2–SrO based nanocomposites and their photocatalytic activity for the treatment of organic pollutants. *J. Mol. Struct.* **2015**, *1098*, 393–399. [CrossRef]
16. Malik, A.; Hameed, S.; Siddiqui, M.J.; Haque, M.M.; Umar, K.; Khan, A.; Muneer, M. Electrical and optical properties of nickel- and molybdenum-doped titanium dioxide nanoparticle: Improved performance in dye-sensitized solar cells. *J. Mater. Eng. Perform.* **2014**, *23*, 3184–3192. [CrossRef]
17. Eslek Koyuncu, D.D.; Okur, M. Removal of AV 90 dye using ordered mesoporous carbon materials prepared via nanocasting of KIT-6: Adsorption isotherms, kinetics and thermodynamic analysis. *Sep. Purif. Technol.* **2021**, *257*, 117657. [CrossRef]
18. Zhang, T.; Wang, W.; Zhao, Y.; Bai, H.; Wen, T.; Kang, S.; Song, G.; Song, S.; Komarneni, S. Removal of heavy metals and dyes by clay-based adsorbents: From natural clays to 1D and 2D nano-composites. *Chem. Eng. J.* **2021**, *420*, 127574. [CrossRef]
19. Mishra, P.; Singh, K.; Dixit, U. Adsorption, kinetics and thermodynamics of phenol removal by ultrasound-assisted sulfuric acid-treated pea (*Pisum sativum*) shells. *Sustain. Chem. Pharm.* **2021**, *22*, 100491. [CrossRef]

20. Wang, L.; Zhang, J.; Zhao, R.; Li, C.; Li, Y.; Zhang, C. Adsorption of basic dyes on activated carbon prepared from *Polygonum orientale* Linn: Equilibrium, kinetic and thermodynamic studies. *Desalination* **2010**, *254*, 68–74. [CrossRef]
21. Mittal, A.; Mittal, J.; Malviya, A.; Kaur, D.; Gupta, V.K. Adsorption of hazardous dye crystal violet from wastewater by waste materials. *J. Colloid Interface Sci.* **2010**, *343*, 463–473. [CrossRef]
22. Amel, K.; Hassen, M.A.; Kerroum, D. Isotherm and kinetics study of biosorption of cationic dye onto banana peel. *Energy Procedia* **2012**, *19*, 286–295. [CrossRef]
23. Khalfaoui, A.; Meniai, A.H. Application of chemically modified orange peels for removal of copper(II) from aqueous solutions. *Theor. Found. Chem. Eng.* **2012**, *46*, 732–739. [CrossRef]
24. Khalfaoui, A.; Bendjamaa, I.; Bensid, T.; Meniai, A.H.; Derbal, K. Effect of calcination on orange peels characteristics: Application of an industrial dye adsorption. *Chem. Eng. Trans.* **2014**, *38*, 361–366. [CrossRef]
25. Mahmoud, M.E.; El-Ghanam, A.M.; Saad, S.R.; Mohamed, R.H.A. Promoted removal of metformin hydrochloride anti-diabetic drug from water by fabricated and modified nanobiochar from artichoke leaves. *Sustain. Chem. Pharm.* **2020**, *18*, 100336. [CrossRef]
26. Imane, B.; Karima, A.; Jamal, M.; Souad, E.H.; Ahmed, M.; Najoua, L. The use and the performance of chemically treated artichoke leaves for textile industrial effluents treatment. *Value Health* **2021**, *31*, 100597. [CrossRef]
27. Saavedra, M.I.; Doval Miñarro, M.; Angosto, J.M.; Fernández-López, J.A. Reuse potential of residues of artichoke (*Cynara scolymus* L.) from industrial canning processing as sorbent of heavy metals in multimetallic effluents. *Ind. Crops Prod.* **2019**, *141*, 111751. [CrossRef]
28. Haque, E.; Jun, J.W.; Jhung, S.H. Adsorptive removal of methyl orange and methylene blue from aqueous solution with a metal-organic framework material, iron terephthalate (MOF-235). *J. Hazard. Mater.* **2011**, *185*, 507–511. [CrossRef]
29. de Oliveira Brito, S.M.; Andrade, H.M.C.; Soares, L.F.; de Azevedo, R.P. Brazil nut shells as a new biosorbent to remove methylene blue and indigo carmine from aqueous solutions. *J. Hazard. Mater.* **2010**, *174*, 84–92. [CrossRef]
30. Wibowo, N.; Setyadhi, L.; Wibowo, D.; Setiawan, J.; Ismadji, S. Adsorption of benzene and toluene from aqueous solutions onto activated carbon and its acid and heat treated forms: Influence of surface chemistry on adsorption. *J. Hazard. Mater.* **2007**, *146*, 237–242. [CrossRef]
31. Loredo-Cancino, M.; Soto-Regalado, E.; Cerino-Córdova, F.J.; García-Reyes, R.B.; García-León, A.M.; Garza-González, M.T. Determining optimal conditions to produce activated carbon from barley husks using single or dual optimization. *J. Environ. Manag.* **2013**, *125*, 117–125. [CrossRef]
32. Saka, C. BET, TG-DTG, FT-IR, SEM, iodine number analysis and preparation of activated carbon from acorn shell by chemical activation with $ZnCl_2$. *J. Anal. Appl. Pyrolysis* **2012**, *95*, 21–24. [CrossRef]
33. Shakoor, S.; Nasar, A. Utilization of punica granatum peel as an eco-friendly biosorbent for the removal of methylene blue dye from aqueous solution. *J. Appl. Biotechnol. Bioeng.* **2018**, *5*, 242–249. [CrossRef]
34. Mahmoud, M.E.; Saad, E.A.; El-Khatib, A.M.; Soliman, M.A.; Allam, E.A.; Fekry, N.A. Green solid synthesis of polyaniline-silver oxide nanocomposite for the adsorptive removal of ionic divalent species of Zn/Co and their radioactive isotopes 65Zn/ 60Co. *Environ. Sci. Pollut. Res.* **2018**, *25*, 22120–22135. [CrossRef] [PubMed]
35. Benalia, A.; Derbal, K.; Panico, A.; Pirozzi, F. Use of acorn leaves as a natural coagulant in a drinking water treatment plant. *Water Res.* **2019**, *11*, 57. [CrossRef]
36. Mashkoor, F.; Nasar, A.; Inamuddin; Asiri, A.M. Exploring the reusability of synthetically contaminated wastewater containing crystal violet dye using tectona grandis sawdust as a very low-cost adsorbent. *Sci. Rep.* **2018**, *8*, 8314. [CrossRef] [PubMed]
37. Shen, J.; Shahid, S.; Amura, I.; Sarihan, A.; Tian, M.; Emanuelsson, E.A. Enhanced adsorption of cationic and anionic dyes from aqueous solutions by polyacid doped polyaniline. *Synth. Met.* **2018**, *245*, 151–159. [CrossRef]
38. Saleh, T.A.; Sarı, A.; Tuzen, M. Effective adsorption of antimony(III) from aqueous solutions by polyamide-graphene composite as a novel adsorbent. *Chem. Eng. J.* **2017**, *307*, 230–238. [CrossRef]
39. Nabili, A.; Fattoum, A.; Passas, R.; Elaloui, E.; Nabili, A. Extraction and characterization of cellulose from date palm (*Phoenix dactylifera* L.). *Cellul. Chem. Technol.* **2014**, *50*, 9–10.
40. Jianxin, H.; Yuyuan, T.; Shan-Yuan, W. Differences in morphological characteristics of bamboo fibres and other natural cellulose fibres: Studies on X-ray diffraction, solid-state 13C-CP/MAS NMR, and second derivative FTIR spectroscopy data. *Iran. Polym. J.* **2007**, *8*, 597–613.
41. Bazan, A.; Nowicki, P.; Półrolniczak, P.; Pietrzak, R. Thermal analysis of activated carbon obtained from residue after supercritical extraction of hops. *J. Therm. Anal. Calorim.* **2016**, *125*, 1199–1204. [CrossRef]
42. Lyu, W.; Yu, M.; Feng, J.; Yan, W. Highly crystalline polyaniline nanofibers coating with low-cost biomass for easy separation and high efficient removal of anionic dye ARG from aqueous solution. *Appl. Surf. Sci.* **2018**, *458*, 413–424. [CrossRef]
43. Roonasi, P.; Holmgren, A. A fourier transform infrared (FTIR) and thermogravimetric analysis (TGA) study of oleate adsorbed on magnetite nano-particle surface. *Appl. Surf. Sci.* **2009**, *255*, 5891–5895. [CrossRef]
44. Khok, Y.T.; Ooi, C.H.; Matsumoto, A.; Yeoh, F.Y. Reactivation of spent activated carbon for glycerine purification. *Adsorption* **2020**, *26*, 1015–1025. [CrossRef]
45. Bencheikh, I.; Azoulay, K.; Mabrouki, J.; El Hajjaji, S.; Dahchour, A.; Moufti, A.; Dhiba, D. The adsorptive removal of MB using chemically treated artichoke leaves: Parametric, kinetic, isotherm and thermodynamic study. *Sci. Afr.* **2020**, *9*, e00509. [CrossRef]

46. Amel, K. Etude Expérimentale de L'élimination de Polluants Organiques et Inorganiques Par Adsorption Sur Des Matériaux Naturels: Application Aux Peaux d'Orange et de Banane. Ph.D. Thesis, University of Constantine, Constantine, Algeria, 2012.
47. Xiao, J.; Lv, W.; Xie, Z.; Tan, Y.; Song, Y.; Zheng, Q. Environmentally friendly reduced graphene oxide as a broad-spectrum adsorbent for anionic and cationic dyes: Via π-π interactions. *J. Mater. Chem. A* **2016**, *4*, 12126–12135. [CrossRef]
48. Afroze, S.; Sen, T.K.; Ang, M.; Nishioka, H. Adsorption of methylene blue dye from aqueous solution by novel biomass eucalyptus sheathiana bark: Equilibrium, kinetics, thermodynamics and mechanism. *Desalin. Water Treat.* **2016**, *57*, 5858–5878. [CrossRef]